

Ebselen Prevents Cigarette Smoke-Induced Cognitive Dysfunction In Mice By Preserving Hippocampal Synaptophysin Expression

Simone N. De Luca

RMIT University

Kurt Brassington

RMIT University

Stanley M. H. Chan

RMIT University

Aleksandar Dobric

RMIT University

Kevin Mou

RMIT University

Huei Jiunn Seow

RMIT University

Ross Vlahos (✉ ross.vlahos@rmit.edu.au)

RMIT University

Research Article

Keywords: cigarette smoking, cessation, neuroinflammation, cognition, antioxidants, synaptogenesis

Posted Date: November 30th, 2021

DOI: <https://doi.org/10.21203/rs.3.rs-1112319/v1>

License:  This work is licensed under a Creative Commons Attribution 4.0 International License.

[Read Full License](#)

Version of Record: A version of this preprint was published at Journal of Neuroinflammation on March 29th, 2022. See the published version at <https://doi.org/10.1186/s12974-022-02432-y>.

Abstract

Background: Cigarette smoking (CS) is the leading cause of chronic obstructive pulmonary disease (COPD). The “spill-over” of pulmonary inflammation into the systemic circulation may damage the brain, leading to cognitive dysfunction. Cessation of CS can improve pulmonary and neurocognitive outcomes, however, its benefit on the neuroinflammatory profile remains uncertain. Here, we investigate how CS exposure impairs neurocognition and whether this can be reversed with CS cessation or an antioxidant treatment.

Methods: Male BALB/c mice were exposed CS (9 cigarettes/day for 8 weeks) followed by 4 weeks of CS cessation. Another cohort of CS-exposed mice were co-administrated with a glutathione peroxidase (Gpx) mimetic, ebselen (10mg/kg) or vehicle (5% CM-cellulose). We assessed pulmonary inflammation, spatial and working memory, and the hippocampal microglial, oxidative and synaptic profiles.

Results: CS exposure increased lung inflammation which was reduced following CS cessation. CS caused spatial and working memory impairments which were attributed to hippocampal microglial activation and suppression of synaptophysin. CS cessation did not improve memory deficits or alter microglial activation. Ebselen completely prevented the CS-induced working and spatial memory impairments, which was associated with restored synaptophysin expression without altering microglial activation.

Conclusion: We were able to model the CS-induced memory impairment and microglial activation seen in human COPD. The preventative effects of ebselen on memory impairment is likely to be dependent on a preserved synaptogenic profile. Cessation alone also appears to be insufficient in correcting the memory impairment, suggesting the importance of incorporating antioxidant therapy to help maximizing the benefit of cessation.

Introduction

Chronic obstructive pulmonary disease (COPD) is a major incurable global health burden affecting 210 million people worldwide and is the 3rd leading cause of death with cigarette smoking (CS) being the major cause in industrialized countries [1]. Noxious particles in CS damage the lung epithelium, driving the recruitment of macrophages, neutrophils, and lymphocytes as well as the release of pro-inflammatory mediators [2-4] and reactive oxygen species (ROS) [5, 6] into the lungs, that drives persisting pulmonary inflammation. Pharmacotherapies targeting oxidative stress, such as the glutathione peroxidase (GPx) mimetic, ebselen, can ameliorate lung inflammation in murine models of COPD [7-10]. It is postulated that injuries of the lung epithelium permits the “spill-over” of pro-inflammatory and oxidative stress mediators into the systemic circulation, leading to secondary medical conditions elsewhere, also known as comorbidities [11].

COPD-induced neurocognitive dysfunction is an emerging area of research which includes alterations in memory, executive functioning and attention [12-14], with up to 61% of people with COPD suffering from neurocognitive dysfunction [12, 15, 16]. Moreover, neurocognitive dysfunction is associated with much of

the disease burden, healthcare utilization and costs, as people with neurocognitive dysfunction often lack adherence to therapeutic interventions and medication, which in turn worsen their COPD morbidity, lead to increased hospitalizations and risk of mortality [12, 17]. Currently, CS cessation is the most effective strategy for improving respiratory symptoms and function in people with COPD [18-21] and may improve cognitive function as soon as two years post-quitting [22-24].

Although the “spill-over” hypothesis may provide an overarching theme for the onset of comorbidities in COPD, the molecular pathway underlying COPD-related neurocognitive dysfunction remain unknown. One possibility is the potential link between CS-induced neurocognitive dysfunction and microglial-mediated neuroinflammation. Microglia are resident immune cells of the brain that modulate and support neurogenesis, synaptogenesis and cognition in healthy individuals [25]. In response to perturbations, microglia undergo morphological transition from a surveillant ramified state to an activated state adapting the ameboid morphology in response to injury, phagocytosing cellular debris [26, 27]. However, chronic activation of microglia can have deleterious effects, promoting neuronal and axonal loss, which would eventuate in neurocognitive dysfunction [28, 29]. Furthermore, studies have shown that microglia are not only sensitive to oxidative stress, but activated microglia are also capable of producing ROS themselves, thereby perpetuating the oxidative burden [30] and neurocognitive dysfunction seen in COPD.

Microglia-driven neuroinflammation is a major mechanism for the cognitive dysfunction, however, whether this type of neuroinflammation is reversible by CS cessation is unknown. Therefore, we investigated the effect of CS cessation on cognition, neuroinflammatory and oxidative stress profiles in the hippocampus of mice to model that of ex-smokers. We also evaluated the effect of co-administration of the antioxidant, ebselen, in memory performance and the neuroinflammatory profile post-CS exposure.

Materials And Methods

Animals

All animal care and experimental procedures were in compliance with the ARRIVE Guidelines [31], Australian Code of Practice for the Care of Experimental Animals and RMIT University Animal Ethics approval (AEC1533). Male BALB/c mice obtained from the Animal Resource Centre (WA, AUS) arrived at 7 weeks of age. The mice were kept under standard laboratory housing conditions, with a 12-hour light/dark cycle, an ambient temperature of 22 °C and *ad libitum* access to water and standard mice chow.

Cigarette smoke exposure and ebselen treatment

Mice were randomly assigned into different experimental groups (n = 14/group) and body weight was recorded every second day. Mice underwent whole body exposure to the smoke of 9 filtered cigarettes (Winfield Red, 16 mg or less of tar, 1.2 mg or less of nicotine), mice exposed to room air (sham) per day for 5 consecutive days a week for 8 weeks as previously published [32, 33]. Cohort 1 consisted of four

groups exposed to CS and one group exposed to room air. Cohort 2 were exposed to CS or room air for 8 weeks with co-administration (oral gavage) of either ebselen (10mg/kg) or 5% CM-cellulose (vehicle). After 8 weeks of exposure, mice were culled by an overdose of anesthetic (Lethobarb, 240 mg/kg; Virbac Pty. Ltd.) or culled after a cessation period of 3, 10 and 33 days.

Bronchoalveolar lavage (BAL) and lung collection

At the end of the study, the lungs were lavaged *in situ* using phosphate buffered saline (PBS) as previously published [7, 32, 34]. BAL fluid (BALF) cytopsin slides were prepared and analyzed; identifying macrophages, neutrophils and lymphocytes using standard morphological criteria. The lungs were then perfused free of blood with PBS, rapidly excised en bloc, blotted and the large left lobe snap frozen for quantitative real-time-PCR (qRT-PCR) analysis.

Brain dissections

Brains were sagittally hemisected and the right hemisphere was excised and the hippocampi was snap-frozen for gene or protein expression (n = 6/group). The left hemisphere was immersed in 4% paraformaldehyde in PBS for 24 h before cryoprotecting in 20% sucrose (n = 6-8/group) for histological analyses. Brains were sectioned into 30 µm coronal sections in a one-in-five series using a cryostat (Leica Biosystems, VIC, AUS).

Gene expression

Total RNA was extracted using RNeasy kits (QIAGEN, CA, USA), then reverse transcribed using a High-Capacity RNA-to-cDNA kit (Life Technologies, CA, USA) prior to real-time PCR analysis (QuantStudio 7, Applied Biosystems, VIC, AUS). All reactions were performed in triplicate, and the data obtained was normalised to *Gapdh* as an endogenous control before analysis using the $\Delta\Delta CT$ method (Supplementary Table 1).

Immunohistochemistry

Coronal sections were blocked for 2 h at room temperature with 3% BSA, 10% NHS, 0.3% Triton X-100 in PBS and incubated in primary antibody (Iba-1: 1:1000, rabbit, Wako Chemicals, VA, USA; RRID: AB_2314666; Synaptophysin: 1:2000, mouse, Sigma-Aldrich, MO, USA; RRID: AB_477523) overnight at 4 °C. Sections were washed in 1xPBS-T then incubated with the fluorescent secondary antibody (1:400, anti-rabbit: Life Technologies, CA, USA; RRID: AB_221544; anti-mouse: Life Technologies, RRID: 2536161) for 2h, mounted and coverslipped with Fluroshield^ä DAPI mounting medium (Sigma-Aldrich). Hippocampal photomicrographs were taken on an upright fluorescent Olympus BX53 microscope (Olympus Corp., Tokyo, Japan). Three sections 60 µm apart between 1.46 and 2.54 mm relative to the bregma were analysed [35]. We assessed Iba-1 images for numbers and area per cell density [25]. For synaptophysin, immunofluorescent intensity was determined via CELLSSENS imaging software (Olympus

Corp). Detection thresholds were set to minimise background fluorescence and allow selection of an area of interest.

Western blot

The right hippocampi from a separate cohort and BALF (n = 6/group), was homogenized (20 µg of total protein or 20µL of BALF) and subjected to either SDS/PAGE using a 10% acrylamide gel or an OxyBlot™ Protein Oxidation Detection Kit (Millipore, MA, USA) [8]. Membranes were incubated overnight (4°C) with primary antibody (anti-Malondialdehyde [MDA]: 1:1000, mouse, Thermo Scientific; RRID: AB_2735263; anti-GAPDH: 1:3000, rabbit, CST, QLD, AUS, RRID: AB_10622025; anti-DNP: 1:300, Millipore) followed by a 2 h incubation with HRP-conjugated secondary antibody (1:1000; CST; RRID: AB_330924). Membranes were then exposed to enhanced chemiluminescence Western Lighting Ultra Solution reagents (Perkin Elmer, MA, USA) and visualised using ChemiDoc (Bio-Rad Laboratories). Relative protein expression was normalised to the band intensity of GAPDH (MDA) or Ponceau S (Sigma-Aldrich) staining.

Neurocognitive assessment

Spontaneous alternation in Y maze (sY-maze): Animals were placed in a Y-maze with spatial cues external to the maze to enable spatial orientation and were freely allowed to explore for 5 min. An arm entry was recorded when the mouse had moved all four paws into an arm. The number of arm entries and the number of sequential entries into all three arms were recorded. The percentage of spontaneous alternation was calculated by dividing the number of alternations by the number of possible alternations.

Novel Object Recognition (NOR): Mice were habituated to the arena for two sessions prior to testing (n = 8-10/ group). Mice were allowed to explore two identical objects placed equally distanced apart (8 min). Following a 1 h inter-trial interval, one object was replaced with a novel object (8 min). The preference index was calculated as time spent interacting with novel object / overall exploration time of the two objects [36, 37]. Total distance was scored using Ethovision (Noldus Information Technology, Wageningen, NL).

Data Analysis

We analyzed the data using a one-way analysis of variance (ANOVA) for cohort 1 and a two-way ANOVA for cohort 2. Where significant differences were found, we performed Tukeys *post-hoc* analysis. Body weights were analyzed using repeated measures (RM) ANOVA with CS as the between factor and day as RM. Pearson's correlation coefficient and regression analysis were used to evaluate the association between protein carbonylation and BALF total cell count, as well as preference index and total locomotor activity in the NOR and sY-maze test. Data are presented as the mean + SEM. Statistical significance was assumed where $p \leq 0.05$.

Results

Smoking cessation restores body weight and reduces BALF cellularity

Similar to previously reported, CS exposure caused a suppression of weight gain when compared to sham mice [7, 32, 33]. Upon cessation, the body weight of the mice rapidly re-bounced and were no different to that of sham-treated at 18 days post-cessation (Fig 1A). CS exposure caused an increase in BALF total cells (Fig 1B), which was attributed to increased macrophage (Fig 1C) and neutrophil recruitment (Fig 1D) but not lymphocytes (Fig 1E). Upon 33 days of cessation, BALF cellularity returned back to sham levels and this positively correlated with reduced BALF protein carbonylation (Fig 1F, G).

Cessation gradually alters the pulmonary inflammatory profile.

CS exposure significantly increased *Tnfa* expression in the lungs when compared to sham mice and this elevated expression was maintained immediately following cessation at both 3- and 10-day time points (Fig 1H). CS prompted an increase in chemokines C-X-C Motif Chemokine Ligand (*Cxcl*)-1, *Cxcl2* and Chemokine ligand 2 (*Ccl2*) expression, however, this subsided back to sham levels following cessation. CS-exposure significantly increased matrix metalloproteinase (*Mmp*)12 expression when compared to sham mice despite a 33-day cessation, while the expression of *Mmp9* was seemingly unaltered by CS or cessation status. *Gpx1* expression was significantly reduced following CS, which persisted following a 33-day cessation, whereas, the expression of *Nox2* was increased following 3 and 10 day cessation but returned to sham level at day 33. Cessation significantly suppressed CS-induced *Nox1* expression, whilst, the CS-induced suppression of *Nox4* was unaltered by cessation.

Hippocampal-dependent working memory persisted despite 33 days CS cessation.

Smoke exposure induced spatial memory impairments, with a reduction in the percentage sY-maze task which remained evident up until 10 days but was resolved by 33 days post-cessation (Fig 2A). CS-exposed mice had a noticeable decrease in arm entries compared to the sham counterparts (Fig 2B), however, there was no correlation between spontaneous alternation and the number of arm entries made (Fig 2C). Moreover, sham mice spent more time exploring the novel object (high preference index) indicating appropriate recall of the NOR task, whereas, CS-exposed mice were unable to differentiate between the novel and familiar object (neutral preference index; Fig 2D, F) suggesting working memory impairment and this was not resolved following a 33-day cessation. The lack of difference in total distance travelled during the NOR task (Fig 2E) is also indicative that the working memory impairment in CS-exposed mice were not associated with an altered locomotor activity.

Prolonged CS cessation induces microglial activation

CS exposure caused an increase in microglial numbers in the CA1 region of the hippocampus when compared to sham mice (Fig 3A); however, did not differ in other regions (Fig 3C, E, G, I). Cessation of 33-days increased Iba-1 positive staining in the molecular region of the dentate gyrus suggesting an increased number of microglia (Fig 3G). CS exposure led to microglial activation as seen by an increased microglial cell area in all regions of the hippocampus (Fig 3). Cessation initially suppressed microglial activation (at day 3 and 10), but eventually resulted in an increased microglial activation (Fig B, D, F, J).

Like that of the lung profile, there was a significant increase in *Mmp12* expression following CS exposure which remained elevated despite CS cessation (Fig 3K).

Cessation was unable to resolve established hippocampal oxidative stress or synaptophysin dysfunction by CS exposure.

Exposure to CS caused an increase in protein carbonylation of hippocampal tissue compared to sham mice (Fig 4A). Similar to the microglial profile, the CS-induced protein carbonylation was initially suppressed but re-emerged following 33 days of cessation. CS exposure caused an increase in MDA expression which was unaltered by cessation (Fig 4B). *Nox1* expression was significantly elevated following 33 days of cessation when compared to sham-exposed mice. Inducible nitric oxide synthase (*iNos*) expression was reduced by CS exposure and eventually normalized to sham level following 33 days of cessation. Like the lung profile, *Gpx1* in CS-exposed and CS cessation mice was suppressed when compared to the shams. The presynaptic protein, synaptophysin, was reduced in the hippocampus of CS-exposed and cessation mice compared to sham mice (Fig 4D).

Ebselen partially resolves CS-induced pulmonary inflammation.

To determine how CS exposure elicits pulmonary inflammation and elevated oxidative stress levels damaging the brain, we pharmacologically targeted oxidative stress using a Gpx mimetic, ebselen, to enhance the removal of ROS. Despite the lack of effects on body weight retention (Fig 5A), ebselen administration markedly attenuated the CS-induced lung inflammation evidenced by the reductions in macrophage and neutrophil recruitments (Fig 5 A-E). To ascertain whether the attenuated inflammation of the lungs was associated with a dampened oxidative stress from ebselen administration, we assessed protein oxidation of the BALF. Our analysis revealed that there was no correlation between protein oxidation and the total number of immune cell infiltration suggesting that both 5% CM cellulose and ebselen was able to antagonize the oxidative burden evoked by CS (Fig 5F).

Ebselen reverses hippocampal-dependent memory impairment following CS exposure

CS exposure reduced the percentage spontaneous alternation suggesting spatial memory impairment, which was completely reversed by ebselen treatment (Fig 6A). CS-exposed mice were also found to have reduced number of arm entries (Fig 6B), but this was unlikely to be a result of reduced locomotor activity, reflected by the lack of correlation between the two (Fig 6C). Moreover, concurrent ebselen treatment with CS exposure was able to completely block the onset of working memory deficits (Fig 6D, F), which was also independent of locomotor activity, suggesting inhibition of oxidative stress protects against hippocampal-dependent memory loss by CS exposure (Fig 6E).

Microglial profiles are unchanged in CS-exposed mice irrespective of ebselen treatment

CS exposure evoked no significant change in microglial number in the hippocampus (Fig 7). Similar to that of the cessation cohort (Fig 3), CS exposure increased microglia area per cell in the CA1 (Fig 7B). In the CA3 and hilus region of the dentate gyrus, CS exposure increased area per cell compared to the sham

mice and this was further augmented by the ebselen treatment (Fig 7D, F). Irrespective of ebselen treatment, CS exposure significantly increased *Tnfa*, *Cxcl1*, *Il1 β* and *Csf1* expressions compared to sham mice, but *Il1 β* and *Mmp9* expression were reduced following ebselen treatment (Fig 7K).

Ebselen treatment preserved synaptophysin expression in the hippocampus

CS exposure alone caused an increase in total protein carbonylation when compared to sham-treated mice (Fig 8A) and ebselen treatment did not resolve this. MDA levels were also enhanced upon CS exposure which returned to sham levels following ebselen treatment (Fig 8B). CS-exposure significantly suppressed *Nox1* and *Nos2* expression when compared to sham mice, which was unaltered by ebselen treatment. Ebselen was able to restore the CS-induced elevations in *Nox4* and *Gpx1* expression to that of sham mice (Fig 8C). Whilst the hippocampal protein carbonylation profile remained elevated, we found that ebselen completely restored the CS-induced reduction in synaptophysin density (Fig 8D, E).

Discussion

The present study suggested that CS exposure caused lung inflammation, hippocampal neuroinflammation, suppression of synaptophysin expression, and spatial and working memory deficits. 33 days of cessation resolved the apparent pulmonary inflammation, however, expression of pro-inflammatory mediators remained elevated in lung tissues, which is consistent with previously published literature [38]. These cognitive deficits and reductions in a key mediator of synaptogenesis. synaptophysin persisted well after cessation, suggesting these alterations to the CNS are not transient and may be responsible for the long-term risk of neurodegenerative diseases. For this reason, we specifically targeted the pulmonary oxidative profile via concomitant ebselen treatment to delineate the role of oxidative stress in cognitive decline. Ebselen completely prevented CS-induced neurocognitive dysfunction and our molecular analysis found that this is attributed to a restoration of synaptophysin.

Smoking cessation studies focusing on cognitive integrity in people with COPD are limited, with many studies excluding participants with COPD from cohort analysis, which could be due to the numerous comorbidities considered as an exclusion criterion [39, 40]. Research has shown that CS cessation in non-COPD participants may increase the risk of accelerated cognitive decline and dementia [23, 39-41]. Two recent studies found that compared with current non-COPD smokers, long-term quitters (> 9 years) had a decreased risk of dementia, however, this is not the case for short-term quitters (< 9 years) [39, 42]. Conversely, others revealed that smokers who had quit for longer than 3 years had reduced risk of dementia comparable with that of never smokers [41]. Others have shown that long-term smoking cessation of greater than 20 years is necessary to fully ameliorate the risk of cognitive impairment and dementia [23, 43]; however, the mechanisms underlying these outcomes remain unclear. We have shown that 8 weeks of CS exposure in BALB/c mice recapitulates key aspects of lung pathologies to that observed in human COPD along with the persistent memory deficits, allowing us to investigate the potential underlying mechanism.

Nicotine is the major psychoactive component of cigarettes involved in the neurobiological effects underlying the sustainment, and reinforcement of smoking. It has become clear that smoking cessation can lead to nicotine withdrawal symptoms including alterations in attention, working and episodic memory, cognitive flexibility and contextual learning processes [44-49]. [45-47]. It is advantageous to consider that previous nicotine studies utilized chronic, continuous administration of nicotine via subcutaneous-implanted osmotic pumps, which is distinctly different from the human smoking pulmonary kinetic pattern and blood concentration of nicotine in smokers [50]. Our study shows a decline in working memory following 8 weeks of CS exposure, which persisted beyond 33 days post-cessation suggesting these neurocognitive impairments may be closer related to pulmonary inflammation elicited by CS rather than nicotine withdrawal symptoms, which have been shown to be fully resolved by 8-days post-nicotine withdrawal. Alongside this, studies have found that CS and e-cigarette cessation for more than 30 days markedly impaired spatial and visual memory [51, 52]. Similarly, mice exposed to nicotine-free e-cigarettes have impaired working memory performance, further emphasising that cognitive impairments may still occur without nicotine [53].

In our model, chronic smoke exposure promoted sustained hippocampal microglial activation that is unaltered by cessation. Consistent with our notion that CS-induced COPD alters the microglial morphology to an ameboid state, an acute treatment of the tobacco-specific procarcinogen compound, 4-N-methyl-N-nitrosamino-1-(3-pyridyl)-1-butanone in mice, for as little as 4 days, can induce robust changes in hippocampal microglial morphology [54]. This reinforces the concept that pulmonary inflammation is likely to be responsible for the activation and modulation of microglial cells. Clinical studies have opposingly shown that smokers have less microglial activation than non-smokers using [11C]DAA1106; a radiotracer for translocator protein (TSPO), an indicator of microglial activation [55-58]. Interestingly, TSPO deficiency suppresses mitochondrial oxidative phosphorylation and glycolysis in mice, resulting in overall mitochondrial dysfunction [59]. Indeed, CS exposure is known to induce a maladaptive mitochondrial hyperfusion response in alveolar epithelial cells [60] and beyond the pulmonary system [61]. Thus, one explanation for the clinical findings is that [11C]DAA1106 is highly metabolised in smokers compared to non-smokers, rather than there being a suppression of microglial activation. Going forward, it will be imperative to evaluate whether pharmacologically targeting microglia both during CS exposure and cessation periods could improve cognitive outcomes. For instance, pharmacological inhibition of microglial activation using minocycline, has been shown to improve cognitive function [62, 63]. Moreover, stable COPD patients given a tetracycline analogue for 4 weeks showed an improvement in lung function and a reduction in systemic inflammation compared to vehicle treated COPD patients, thus, it may be capable of attenuating neuroinflammation [64].

Oxidative stress is a key driver of CS-induced lung damage and has recently been proposed as a fundamental driver of neurodegeneration and cognitive dysfunction [65], however, there is limited literature on the impact of CS-induced oxidative stress in the brain. We show that cognitive impairment is associated with elevated levels of protein carbonylation and lipid peroxidation as well as down-regulated *Gpx1* expression in the hippocampus of CS exposed and CS cessation mice. Studies have shown increased gene expression of pro-oxidants such as *iNos*, *Nox4*, and *Nox2* in the whole brain following CS

exposure, which are typically triggered as a secondary response to oxidative stress [66]. Moreover, CS exposure induces a reduction of cytoplasmic staining of transcription factor Nrf2 (nuclear factor [erythroid-derived 2]-like 2) in rats [66] and mice [67] which is a master regulator of a myriad of cellular antioxidants, thus suggesting the dual action of CS exposure on enhancing oxidant generation and suppression of cellular defence.

Given that excessive oxidative stress is often linked to microglial activation [68] and that microglial cells are a major cellular source of ROS under inflammatory states [69, 70], it is tempting to speculate that a prophylactic antioxidant treatment may attenuate the oxidative burden and improve CS-induced cognitive dysfunction. A prophylactic treatment with selenium and Vitamin E concomitant with CS exposure for 20 weeks was sufficient to prevent impairments in whole brain's antioxidant defence system [71]. It must be noted that previous studies have assessed whole brain tissue, rather than individual regions. We found that hippocampal lipid peroxidation is significantly reduced following antioxidant treatment, however, protein carbonylation is not. The hippocampus is highly susceptible to oxidative insults [72], thus, it seems highly plausible that ebselen may be able to reduce the CS-induced oxidative burden globally, however, hippocampal oxidative stress may remain elevated alongside the elevated microglial profile. This is not unprecedented given that the attenuation of pulmonary inflammation following ebselen administration is largely due to a reduction in neutrophilic infiltration [7, 10], leading us to postulate that ebselen's memory enhancing ability may be exerted via a microglial-independent mechanism which targets synaptic integrity in smokers. Synapses are formed by the functional contact of presynaptic axonal terminals with postsynaptic dendritic processes allowing for the efficient transmission of signal [73, 74]. It is apparent that aberrant synaptic plasticity, due to abnormal expression of synaptophysin and the postsynaptic scaffolding protein, PSD-95, in the hippocampus, is functionally related to cognitive decline and Alzheimer's Disease [75-77]. The loss of pre/post synaptic proteins, progressive loss of synaptic density and the subsequent cognitive decline is typified by an increase in reactive astrocytic expression, alongside microglial activation [78, 79]. We, and others, have demonstrated that CS exposure induces a loss of synaptic integrity, via a reduction in synaptophysin in the hilus region of the dentate gyrus [80] and importantly this is not reversible even after 33 days CS cessation. Moreover, concomitant ebselen treatment prevented the loss of synaptic integrity by retaining synaptophysin density in CS-exposed mice to that of sham mice.

CS cessation remains one of the most effective strategies for preventing and reducing the progressive decline in lung function attributable to COPD [18-21, 81, 82]. Clinical research indicates that long-term non-COPD quitters have improved cognitive integrity compared to current smokers [22-24, 41]. We are the first to show that neuroinflammation persists in spite of cessation and this is associated with continuous cognitive impairments, even when pulmonary inflammation has subsided. Moreover, we demonstrate that a prophylactic pharmacological treatment with ebselen can preserve cognitive function and prevent the loss of synaptophysin, despite the sustained microglial activation following CS exposure. Mitigating the pulmonary inflammation and the potential "spill-over" into the CNS could halt the neuroinflammatory profile and the associated cognitive decline in CS-induced COPD. Therefore, it is clear from our study that CS cessation alone is not enough to improve neuroinflammation and cognition and that future research

should focus on investigating CS cessation with concomitant pharmacological interventions, particularly antioxidants, which we have shown to target both pulmonary and systemic inflammation and the associated neurological comorbidities.

Abbreviations

ANOVA: analyses of variance; BAL: bronchoalveolar lavage; BALF: bronchoalveolar lavage fluid; Ccl: C-C Motif Chemokine Ligand; COPD: chronic obstructive pulmonary disease; CS: cigarette smoke; Cxcl: C-X-C Motif Chemokine Ligand; Gpx: Glutathione peroxidase; IL: interleukin; iNOS: inducible nitric oxide synthase; MDA: Malondialdehyde; Mmp: Matrix Metalloproteinase; NOR: novel object recognition; NOX: NADPH oxidase; qRT-PCR: quantitative real-time-PCR; RM: repeated measures; ROS: reactive oxygen species; sY-maze: spontaneous alternation in the Y-maze; Tnf: tumor necrosis factor; TSPO: Translocator protein.

Declarations

Ethics approval

We conducted all procedures in accordance with the National Health and Medical Research Council Australia Code of Practice for the Care of Experimental Animals and the RMIT University Animal Ethics Committee approval (AEC1533).

Consent for publication

Not applicable.

Availability of data and materials

The datasets supporting the conclusions of this article are available upon request.

Competing interests

The authors declare that they have no competing interests.

Funding

This study was supported by the National Health and Medical Research Council of Australia [Project Grant ID1139843] and Lung Foundation Australia / Boehringer Ingelheim Fellowship awarded to Dr De Luca.

Authors' contributions

RV and SND designed the study. SND co-ordinated the animal work, carried out the study, analysed the data, and wrote the manuscript. KB, SMHC, AD, KM, and HJS carried out the study and edited the

manuscript. All authors read and approved the final manuscript.

References

1. Vogelmeier CF, Criner GJ, Martinez FJ, Anzueto A, Barnes PJ, Bourbeau J, Celli BR, Chen R, Decramer M, Fabbri LM, et al: **Global Strategy for the Diagnosis, Management, and Prevention of Chronic Obstructive Lung Disease 2017 Report. GOLD Executive Summary.** *Am J Respir Crit Care Med* 2017, **195**:557-582.
2. Barnes PJ, Shapiro SD, Pauwels RA: **Chronic obstructive pulmonary disease: molecular and cellular mechanisms.** *Eur Respir J* 2003, **22**:672-688.
3. Vlahos R, Bozinovski S: **Recent advances in pre-clinical mouse models of COPD.** *Clin Sci* 2014, **126**:253-265.
4. Bozinovski S, Seow HJ, Chan SP, Anthony D, McQualter J, Hansen M, Jenkins BJ, Anderson GP, Vlahos R: **Innate cellular sources of interleukin-17A regulate macrophage accumulation in cigarette- smoke-induced lung inflammation in mice.** *Clin Sci* 2015, **129**:785-796.
5. Rahman I, Morrison D, Donaldson K, MacNee W: **Systemic oxidative stress in asthma, COPD, and smokers.** *Am J Respir Crit Care Med* 1996, **154**:1055-1060.
6. Bernardo I, Bozinovski S, Vlahos R: **Targeting oxidant-dependent mechanisms for the treatment of COPD and its comorbidities.** *Pharmacol Ther* 2015, **155**:60-79.
7. Brassington K, Chan SMH, Seow HJ, Dobric A, Bozinovski S, Selemidis S, Vlahos R: **Ebselen reduces cigarette smoke-induced vascular endothelial dysfunction in mice.** *Br J Pharmacol* 2021, **178**:1805-1818.
8. Chan SMH, Bernardo I, Mastronardo C, Mou K, De Luca SN, Seow HJ, Dobric A, Brassington K, Selemidis S, Bozinovski S, Vlahos R: **Apocynin prevents cigarette smoking-induced loss of skeletal muscle mass and function by preserving proteostatic signalling.** *Br J Pharmacol* 2021, **178**:3049-3066.
9. Duong C, Seow HJ, Bozinovski S, Crack PJ, Anderson GP, Vlahos R: **Glutathione peroxidase-1 protects against cigarette smoke-induced lung inflammation in mice.** *Am J Physiol Lung Cell Mol Physiol* 2010, **299**:L425-433.
10. Oostwoud LC, Gunasinghe P, Seow HJ, Ye JM, Selemidis S, Bozinovski S, Vlahos R: **Apocynin and ebselen reduce influenza A virus-induced lung inflammation in cigarette smoke-exposed mice.** *Sci Rep* 2016, **6**:20983.
11. Barnes PJ, Celli BR: **Systemic manifestations and comorbidities of COPD.** *Eur Respir J* 2009, **33**:1165-1185.
12. Dodd JW: **Lung disease as a determinant of cognitive decline and dementia.** *Alzheimers Res The* 2015, **7**:32-32.

13. Yazar EE, Aydin S, Gunluoglu G, Kamat S, Gungen AC, Yildiz P: **Clinical effects of cognitive impairment in patients with chronic obstructive pulmonary disease.** *Chronic Respir Dis* 2018, **15**:306-314.
14. Shehata MEDA, Samaha HMS, Elsaid AR, Helmy EM, Mustafa W: **Magnetic resonance apparent diffusion coefficient values of the brain in COPD.** *Egypt J Chest Dis Tuberc* 2017, **66**:237-242.
15. Yohannes AM, N Eakin M, Holbrook JT, Sugar EA, Henderson R, Baker AM, Casper AS, Kaminsky DA, Rea AL, Mathews AM, et al: **Association of mild cognitive impairment and characteristic of COPD and overall health status in a cohort study.** *Expert Rev Respir Med* 2021, **15**:153-159.
16. France G, Orme MW, Greening NJ, Steiner MC, Chaplin EJ, Clinch L, Singh SJ: **Cognitive function following pulmonary rehabilitation and post-discharge recovery from exacerbation in people with COPD.** *Respir Med* 2021, **176**:106249.
17. Antonelli-Incalzi R, Corsonello A, Pedone C, Trojano L, Acanfora D, Spada A, Izzo O, Rengo F: **Drawing impairment predicts mortality in severe COPD.** *Chest* 2006, **130**:1687-1694.
18. Tashkin DP: **Smoking Cessation in Chronic Obstructive Pulmonary Disease.** *Semin Respir Crit Care Med* 2015, **36**:491-507.
19. Warnier MJ, van Riet EE, Rutten FH, De Bruin ML, Sachs AP: **Smoking cessation strategies in patients with COPD.** *Eur Respir J* 2013, **41**:727-734.
20. Godtfredsen NS, Lam TH, Hansel TT, Leon ME, Gray N, Dresler C, Burns DM, Prescott E, Vestbo J: **COPD-related morbidity and mortality after smoking cessation: status of the evidence.** *Eur Respir J* 2008, **32**:844-853.
21. Liang J, Abramson MJ, Zwar NA, Russell GM, Holland AE, Bonevski B, Mahal A, Phillips K, Eustace P, Paul E, et al: **Diagnosing COPD and supporting smoking cessation in general practice: evidence-practice gaps.** *Med J Aust* 2018, **208**:29-34.
22. Sabia S, Elbaz A, Dugravot A, Head J, Shipley M, Hagger-Johnson G, Kivimaki M, Singh-Manoux A: **Impact of smoking on cognitive decline in early old age: the Whitehall II cohort study.** *Arch Gen Psychiatry* 2012, **69**:627-635.
23. Hu M, Yin H, Shu X, Jia Y, Leng M, Chen L: **Multi-angles of smoking and mild cognitive impairment: is the association mediated by sleep duration?** *Neurol Sci* 2019, **40**:1019-1027.
24. Almeida OP, Garrido GJ, Alfonso H, Hulse G, Lautenschlager NT, Hankey GJ, Flicker L: **24-month effect of smoking cessation on cognitive function and brain structure in later life.** *Neuroimage* 2011, **55**:1480-1489.
25. De Luca SN, Soch A, Sominsky L, Nguyen T-X, Bosakhar A, Spencer SJ: **Glial remodeling enhances short-term memory performance in Wistar rats.** *J Neuroinflam* 2020, **17**:52-52.

26. Nimmerjahn A, Kirchhoff F, Helmchen F: **Resting microglial cells are highly dynamic surveillants of brain parenchyma in vivo.** *Science* 2005, **308**:1314-1318.
27. Davalos D, Grutzendler J, Yang G, Kim JV, Zuo Y, Jung S, Littman DR, Dustin ML, Gan WB: **ATP mediates rapid microglial response to local brain injury in vivo.** *Nature Neuroscience* 2005, **8**:752-758.
28. Lehnardt S, Massillon L, Follett P, Jensen FE, Ratan R, Rosenberg PA, Volpe JJ, Vartanian T: **Activation of innate immunity in the CNS triggers neurodegeneration through a Toll-like receptor 4-dependent pathway.** *PNAS* 2003, **100**:8514-8519.
29. Banati RB, Gehrmann J, Schubert P, Kreutzberg GW: **Cytotoxicity of microglia.** *Glia* 1993, **7**:111-118.
30. Lull ME, Block ML: **Microglial activation and chronic neurodegeneration.** *Neurotherapeutics* 2010, **7**:354-365.
31. Percie du Sert N, Hurst V, Ahluwalia A, Alam S, Avey MT, Baker M, Browne WJ, Clark A, Cuthill IC, Dirnagl U, et al: **The ARRIVE guidelines 2.0: Updated guidelines for reporting animal research.** *Experiment Physiol* 2020, **105**:1459-1466.
32. Vlahos R, Bozinovski S, Jones JE, Powell J, Gras J, Lilja A, Hansen MJ, Gualano RC, Irving L, Anderson GP: **Differential protease, innate immunity, and NF-kappaB induction profiles during lung inflammation induced by subchronic cigarette smoke exposure in mice.** *Am J Physiol Lung Cell Mol Physiol* 2006, **290**:L931-945.
33. Chan SMH, Cerni C, Passey S, Seow HJ, Bernardo I, Poel Cvd, Dobric A, Brassington K, Selemidis S, Bozinovski S, Vlahos R: **Cigarette Smoking Exacerbates Skeletal Muscle Injury Without Compromising its Regenerative Capacity.** *Am J Respir Cell Mol* 2020, **62**:217-230.
34. Hepworth ML, Passey SL, Seow HJ, Vlahos R: **Losartan does not inhibit cigarette smoke-induced lung inflammation in mice.** *Sci Rep* 2019, **9**:15053.
35. Franklin KBJ, Paxinos G: **The Mouse Brain in Stereotaxic Coordinates.** *Elsevier* 2005, **Compact second edition.**
36. Hammond RS, Tull LE, Stackman RW: **On the delay-dependent involvement of the hippocampus in object recognition memory.** *Neurobiol Learn Mem* 2004, **82**:26-34.
37. Antunes M, Biala G: **The novel object recognition memory: neurobiology, test procedure, and its modifications.** *Cogn Process* 2012, **13**.
38. De Cunto G, Bartalesi B, Cavarra E, Balzano E, Lungarella G, Lucattelli M: **Ongoing Lung Inflammation and Disease Progression in Mice after Smoking Cessation: Beneficial Effects of Formyl-Peptide Receptor Blockade.** *Am J Pathol* 2018, **188**:2195-2206.

39. Deal JA, Power MC, Palta P, Alonso A, Schneider ALC, Perryman K, Bandeen-Roche K, Sharrett AR: **Relationship of Cigarette Smoking and Time of Quitting with Incident Dementia and Cognitive Decline.** *J Am Geriatr Soc* 2020, **68**:337-345.
40. Noé-Díaz V, Salinas-Rivera E, Cruz-Pérez F, García-Gómez LA, Mandujano-Baeza E, Ortiz-Moncada G, Ramírez-Venegas A, Sansores RH: **Changes on executive functions before and after quitting smoking: Pilot study.** *JSubst Use* 2018, **23**:452-456.
41. Lu Y, Sugawara Y, Zhang S, Tomata Y, Tsuji I: **Smoking cessation and incident dementia in elderly Japanese: the Ohsaki Cohort 2006 Study.** *Eur J Epidemiol* 2020, **35**:851-860.
42. Choi D, Choi S, Park SM: **Effect of smoking cessation on the risk of dementia: a longitudinal study.** *Ann Clin Transl Neurol* 2018, **5**:1192-1199.
43. Mons U, Schöttker B, Müller H, Kliegel M, Brenner H: **History of lifetime smoking, smoking cessation and cognitive function in the elderly population.** *Eur J Epidemiol* 2013, **28**:823-831.
44. Patterson F, Jepson C, Loughhead J, Perkins K, Strasser AA, Siegel S, Frey J, Gur R, Lerman C: **Working memory deficits predict short-term smoking resumption following brief abstinence.** *Drug Alcohol Depend* 2010, **106**:61-64.
45. Saravia R, Flores A, Plaza-Zabala A, Busquets-Garcia A, Pastor A, de la Torre R, Di Marzo V, Marsicano G, Ozaita A, Maldonado R, Berrendero F: **CB1 Cannabinoid Receptors Mediate Cognitive Deficits and Structural Plasticity Changes During Nicotine Withdrawal.** *Biol Psychiatry* 2017, **81**:625-634.
46. Saravia R, Ten-Blanco M, Grande MT, Maldonado R, Berrendero F: **Anti-inflammatory agents for smoking cessation? Focus on cognitive deficits associated with nicotine withdrawal in male mice.** *Brain Behav Immun* 2019, **75**:228-239.
47. Cole RD, Zimmerman M, Matchanova A, Kutlu MG, Gould TJ, Parikh V: **Cognitive rigidity and BDNF-mediated frontostriatal glutamate neuroadaptations during spontaneous nicotine withdrawal.** *Neuropsychopharmacology* 2020, **45**:866-876.
48. Gould TJ, Wilkinson DS, Yildirim E, Blendy JA, Adoff MD: **Dissociation of tolerance and nicotine withdrawal-associated deficits in contextual fear.** *Brain Res* 2014, **1559**:1-10.
49. Semenova S, Stolerman IP, Markou A: **Chronic nicotine administration improves attention while nicotine withdrawal induces performance deficits in the 5-choice serial reaction time task in rats.** *Pharmacol Biochem Behav* 2007, **87**:360-368.
50. Shao XM, Xu B, Liang J, Xie XS, Zhu Y, Feldman JL: **Nicotine delivery to rats via lung alveolar region-targeted aerosol technology produces blood pharmacokinetics resembling human smoking.** *Nicotine Tob Res* 2013, **15**:1248-1258.

51. Ponzoni L, Braida D, Carboni L, Moretti M, Viani P, Clementi F, Zoli M, Gotti C, Sala M: **Persistent cognitive and affective alterations at late withdrawal stages after long-term intermittent exposure to tobacco smoke or electronic cigarette vapour. Behavioural changes and their neurochemical correlates.** *Pharmacol Res* 2020, **158**:104941.
52. Ponzoni L, Moretti M, Sala M, Fasoli F, Mucchietto V, Lucini V, Cannazza G, Gallesi G, Castellana CN, Clementi F, et al: **Different physiological and behavioural effects of e-cigarette vapour and cigarette smoke in mice.** *Eur Neuropsychopharmacol* 2015, **25**:1775-1786.
53. Heldt NA, Seliga A, Winfield M, Gajghate S, Reichenbach N, Yu X, Rom S, Tenneti A, May D, Gregory BD, Persidsky Y: **Electronic cigarette exposure disrupts blood-brain barrier integrity and promotes neuroinflammation.** *Brain Behav Immun* 2020, **88**:363-380.
54. Ghosh D, Mishra MK, Das S, Kaushik DK, Basu A: **Tobacco carcinogen induces microglial activation and subsequent neuronal damage.** *J Neurochem* 2009, **110**:1070-1081.
55. Brody AL, Gehlbach D, Garcia LY, Enoki R, Hoh C, Vera D, Kotta KK, London ED, Okita K, Nurmi EL, et al: **Effect of overnight smoking abstinence on a marker for microglial activation: a [(11)C]DAA1106 positron emission tomography study.** *Psychopharmacology* 2018, **235**:3525-3534.
56. Brody AL, Hubert R, Enoki R, Garcia LY, Mamoun MS, Okita K, London ED, Nurmi EL, Seaman LC, Mandelkern MA: **Effect of Cigarette Smoking on a Marker for Neuroinflammation: A [(11)C]DAA1106 Positron Emission Tomography Study.** *Neuropsychopharmacology* 2017, **42**:1630-1639.
57. Rupprecht R, Papadopoulos V, Rammes G, Baghai TC, Fan J, Akula N, Groyer G, Adams D, Schumacher M: **Translocator protein (18 kDa) (TSPO) as a therapeutic target for neurological and psychiatric disorders.** *Nat Rev Drug Discov* 2010, **9**:971-988.
58. Venneti S, Lopresti BJ, Wang G, Slagel SL, Mason NS, Mathis CA, Fischer ML, Larsen NJ, Mortimer AD, Hastings TG, et al: **A comparison of the high-affinity peripheral benzodiazepine receptor ligands DAA1106 and (R)-PK11195 in rat models of neuroinflammation: implications for PET imaging of microglial activation.** *J Neurochem* 2007, **102**:2118-2131.
59. Yao R, Pan R, Shang C, Li X, Cheng J, Xu J, Li Y: **Translocator Protein 18 kDa (TSPO) Deficiency Inhibits Microglial Activation and Impairs Mitochondrial Function.** *Front Pharmacol* 2020, **11**.
60. Ballweg K, Mutze K, Königshoff M, Eickelberg O, Meiners S: **Cigarette smoke extract affects mitochondrial function in alveolar epithelial cells.** *Am J Physiol Lung Cell Mol Physiol* 2014, **307**:L895-L907.
61. Dikalov S, Itani H, Richmond B, Arslanbaeva L, Vergeade A, Rahman SMJ, Boutaud O, Blackwell T, Massion PP, Harrison DG, Dikalova A: **Tobacco smoking induces cardiovascular mitochondrial oxidative**

stress, promotes endothelial dysfunction, and enhances hypertension. *Am J Physiol Heart Circ Physiol* 2019, **316**:H639-H646.

62. Cope EC, LaMarca EA, Monari PK, Olson LB, Martinez S, Zych AD, Katchur NJ, Gould E: **Microglia play an active role in obesity-associated cognitive decline.** *J Neurosci* 2018:0789-0718.

63. Jiang Y, Liu Y, Zhu C, ma X, Ma L, Zhou L, Huang Q, Cen L, Pi R: **Minocycline enhances hippocampal memory, neuroplasticity and synapse-associated proteins in aged C57 BL/6 mice.** *Neurobiol Learn Mem* 2015, **121**.

64. Dalvi PS, Singh A, Trivedi HR, Ghanchi FD, Parmar DM, Mistry SD: **Effect of doxycycline in patients of moderate to severe chronic obstructive pulmonary disease with stable symptoms.** *Ann Thorac Med* 2011, **6**:221-226.

65. Kandlur A, Satyamoorthy K, Gangadharan G: **Oxidative Stress in Cognitive and Epigenetic Aging: A Retrospective Glance.** *Front Mol Neurosci* 2020, **13**.

66. Khanna A, Guo M, Mehra M, Royal W, 3rd: **Inflammation and oxidative stress induced by cigarette smoke in Lewis rat brains.** *J Neuroimmunol* 2013, **254**:69-75.

67. Sivandzade F, Alqahtani F, Sifat A, Cucullo L: **The cerebrovascular and neurological impact of chronic smoking on post-traumatic brain injury outcome and recovery: an in vivo study.** *J Neuroinflam* 2020, **17**:133.

68. Ding X, Zhang M, Gu R, Xu G, Wu H: **Activated microglia induce the production of reactive oxygen species and promote apoptosis of co-cultured retinal microvascular pericytes.** *Graefes Arch Clin Exp Ophthalmol* 2017, **255**:777-788.

69. Brown GC, Neher JJ: **Inflammatory neurodegeneration and mechanisms of microglial killing of neurons.** *Mol Neurobiol* 2010, **41**:242-247.

70. Sierra A, Navascués J, Cuadros MA, Calvente R, Martín-Oliva D, Ferrer-Martín RM, Martín-Estebané M, Carrasco MC, Marín-Teva JL: **Expression of inducible nitric oxide synthase (iNOS) in microglia of the developing quail retina.** *PLoS One* 2014, **9**:e106048.

71. Ozkan A, Fiskin K, Ayhan AG: **Effect of vitamin E and selenium on antioxidant enzymes in brain, kidney and liver of cigarette smoke-exposed mice.** *Biologia* 2007, **62**:360-364.

72. Salim S: **Oxidative Stress and the Central Nervous System.** *J Pharmacol Exp Ther* 2017, **360**:201-205.

73. Masliah E, Mallory M, Alford M, DeTeresa R, Hansen LA, McKeel DW, Jr., Morris JC: **Altered expression of synaptic proteins occurs early during progression of Alzheimer's disease.** *Neurology* 2001, **56**:127-129.

74. Coley AA, Gao WJ: **PSD-95 deficiency disrupts PFC-associated function and behavior during neurodevelopment.** *Sci Rep* 2019, **9**.
75. Deng XH, Ai WM, Lei DL, Luo XG, Yan XX, Li Z: **Lipopolysaccharide induces paired immunoglobulin-like receptor B (PirB) expression, synaptic alteration, and learning-memory deficit in rats.** *Neuroscience* 2012, **209**:161-170.
76. Schmitt U, Tanimoto N, Seeliger M, Schaeffel F, Leube RE: **Detection of behavioral alterations and learning deficits in mice lacking synaptophysin.** *Neuroscience* 2009, **162**:234-243.
77. Xie Y, Tan Y, Zheng Y, Du X, Liu Q: **Ebselen ameliorates β -amyloid pathology, tau pathology, and cognitive impairment in triple-transgenic Alzheimer's disease mice.** *J Biol Inorg Chem* 2017, **22**:851-865.
78. Zhang X, Shen X, Dong J, Liu W-C, Song M, Sun Y, Shu H, Towse C-L, Liu W, Liu C-F, Jin X: **Inhibition of Reactive Astrocytes with Fluorocitrate Ameliorates Learning and Memory Impairment Through Upregulating CRTAC1 and Synaptophysin in Ischemic Stroke Rats.** *Cell Mol Neurobiol* 2019, **39**:1151-1163.
79. Chen YY, Zhang L, Shi DL, Song XH, Shen YL, Zheng MZ, Wang LL: **Resveratrol Attenuates Subacute Systemic Inflammation-Induced Spatial Memory Impairment via Inhibition of Astrocyte Activation and Enhancement of Synaptophysin Expression in the Hippocampus.** *Ann Clin Lab Sci* 2017, **47**:17-24.
80. Ho Y-S, Yang X, Yeung S-C, Chiu K, Lau C-F, Tsang AW-T, Mak JC-W, Chang RC-C: **Cigarette Smoking Accelerated Brain Aging and Induced Pre-Alzheimer-Like Neuropathology in Rats.** *Plos One* 2012, **7**:e36752.
81. Scanlon PD, Connett JE, Waller LA, Altose MD, Bailey WC, Buist AS, Tashkin DP: **Smoking cessation and lung function in mild-to-moderate chronic obstructive pulmonary disease. The Lung Health Study.** *Am J Respir Crit Care Med* 2000, **161**:381-390.
82. Pelkonen M, Notkola IL, Tukiainen H, Tervahauta M, Tuomilehto J, Nissinen A: **Smoking cessation, decline in pulmonary function and total mortality: a 30 year follow up study among the Finnish cohorts of the Seven Countries Study.** *Thorax* 2001, **56**:703-707.

Figures

Figure 1

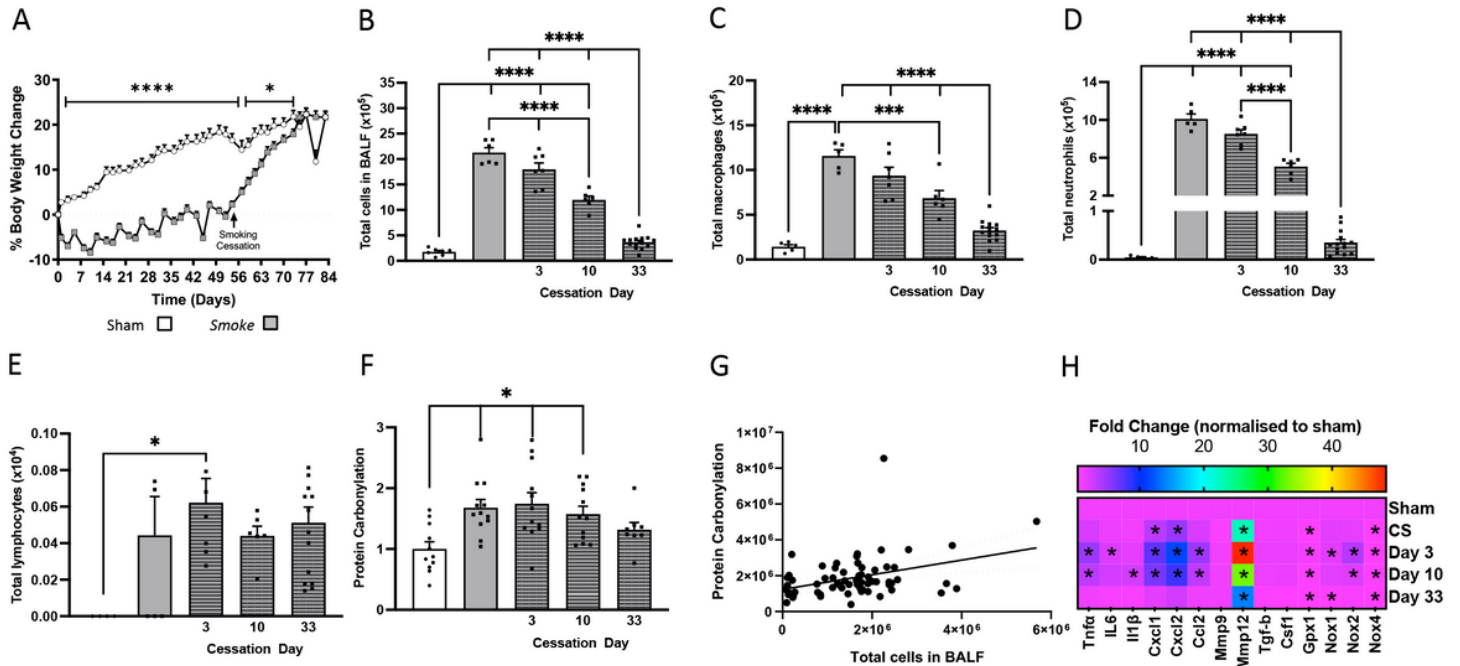


Figure 1

Cigarette smoke (CS)-induced weight loss and bronchoalveolar lavage fluid (BALF) cellularity was reversed 33 days after CS cessation. Mice were exposed to CS or room air (sham) for 8 weeks. CS exposure was then stopped, and mice were housed for an additional 3, 10 or 33 days. (A) body weight percentage change (exposure by day interaction: $F(37,888) = 54.87$, $p < 0.0001$; $n=14$ per group). (B) Total number of cells ($F(4,35) = 146.1$, $p < 0.0001$); (C) macrophages ($F(4,32) = 41.88$, $p < 0.0001$); (D) neutrophils ($F(4,35) = 272.5$, $p < 0.0001$); (E) lymphocytes in BALF ($n=6-10$ per group). (F) BALF Protein Carbonylation ($F(4,50) = 4.553$, $p < 0.003$) and (G) BALF Protein Carbonylation correlation ($r(62) = 0.1350$, $p = 0.0028$; $n = 6$ per group). (H) Gene expression of cytokines and chemokines in the lung (tumor necrosis factor [Tnf]: $F(4,23) = 24.11$, $p < 0.0001$; interleukin 6 [Il6]: $F(4,25) = 4.03$, $p = 0.011$; Il1b: $F(4,25) = 5.83$, $p = 0.002$; C-X-C Motif Chemokine Ligand [Cxcl]-1: $F(4,23) = 7.90$, $p = 0.0004$; Cxcl2: $F(4,21) = 61.69$, $p < 0.0001$; C-C Motif Chemokine Ligand 2 [CCL2]: $F(4,23) = 24.11$, $p < 0.0001$; Matrix Metalloproteinase [Mmp]12: $F(4,23) = 24.57$, $p < 0.0001$; Glutathione peroxidase [Gpx]1: $F(4,23) = 4.929$, $p = 0.0051$; NADPH oxidase [Nox]2: $F(4,23) = 25.42$, $p < 0.0001$; Nox1: $F(4,24) = 9.292$, $p < 0.0001$; Nox4: ($F(4,25) = 6.360$, $p = 0.0011$). Data are expressed as mean + SEM. * $p < 0.05$, *** $p < 0.001$, **** $p < 0.0001$.

Figure 2

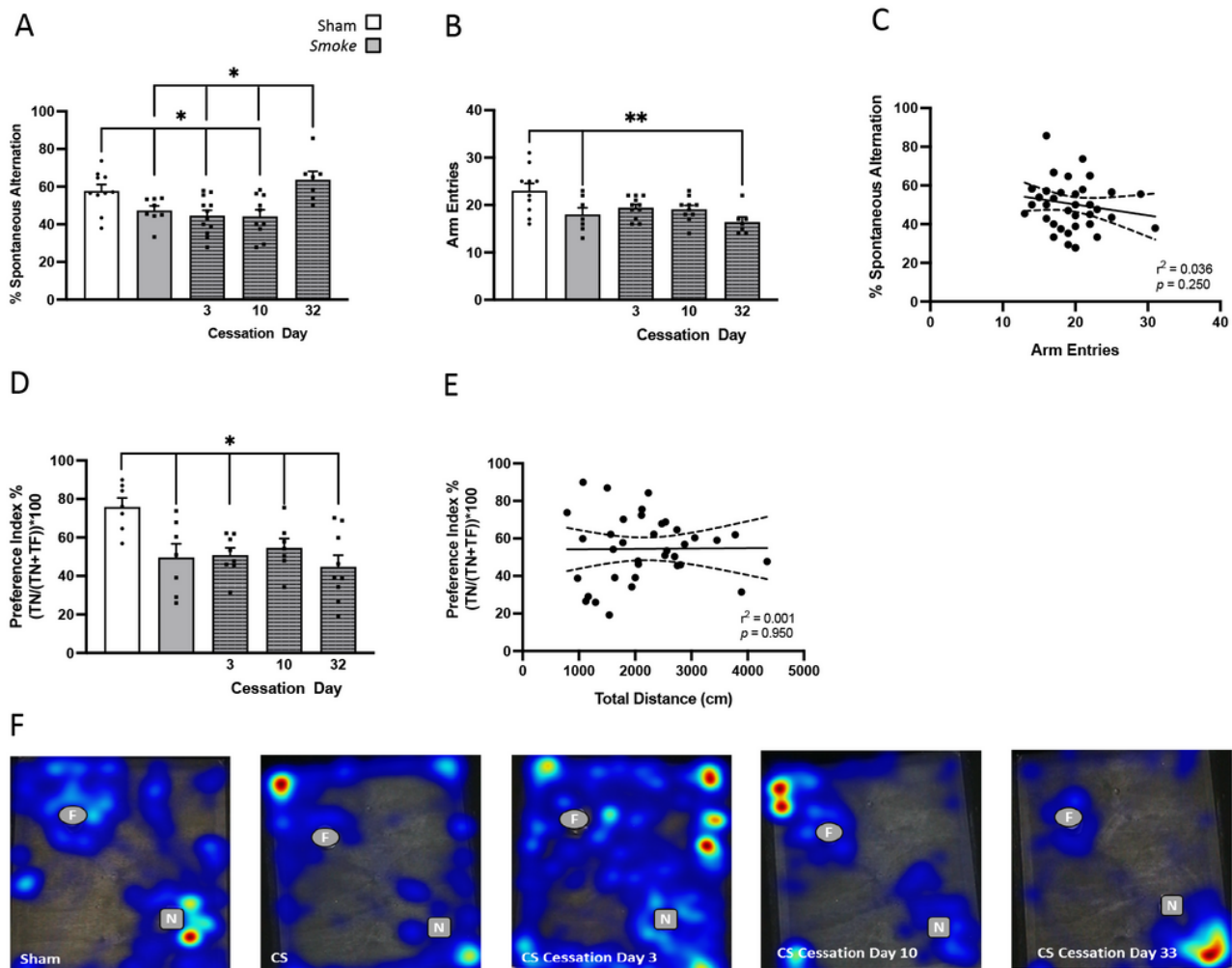


Figure 2

Cigarette smoke (CS) cessation reverses hippocampal-dependent spatial but not working memory impairments. (A) spontaneous alternation percentage in Y-maze ($F(4,42) = 6.340$, $p = 0.0004$; $n = 7 - 11$); (B) Y-maze arm entries ($F(4,40) = 4.482$, $p = 0.0004$); (C) correlation between arm entries and spontaneous alternation in Y-maze ($r(43) = 0.0306$, $p = 0.250$); (D) novel objection recognition (NOR) task preference index ($F(4,33) = 4.829$, $p = 0.0035$; $n = 7 - 9$); (E) correlation between preference index and total distance (cm) in mice exposed to room air (sham), CS or CS cessation for either 3 days, 10 days or 33 days ($r(34) = 0.0001$, $p = 0.953$); (F) heatmaps illustrating familiar object (circle) and novel object (square) exploration in the NOR. Heatmaps were generated in Ethovision using the over-heatmap setting

allowing comparison between the representative animals. Data are expressed as mean + SEM. * $p < 0.05$, ** $p < 0.01$.

Figure 3

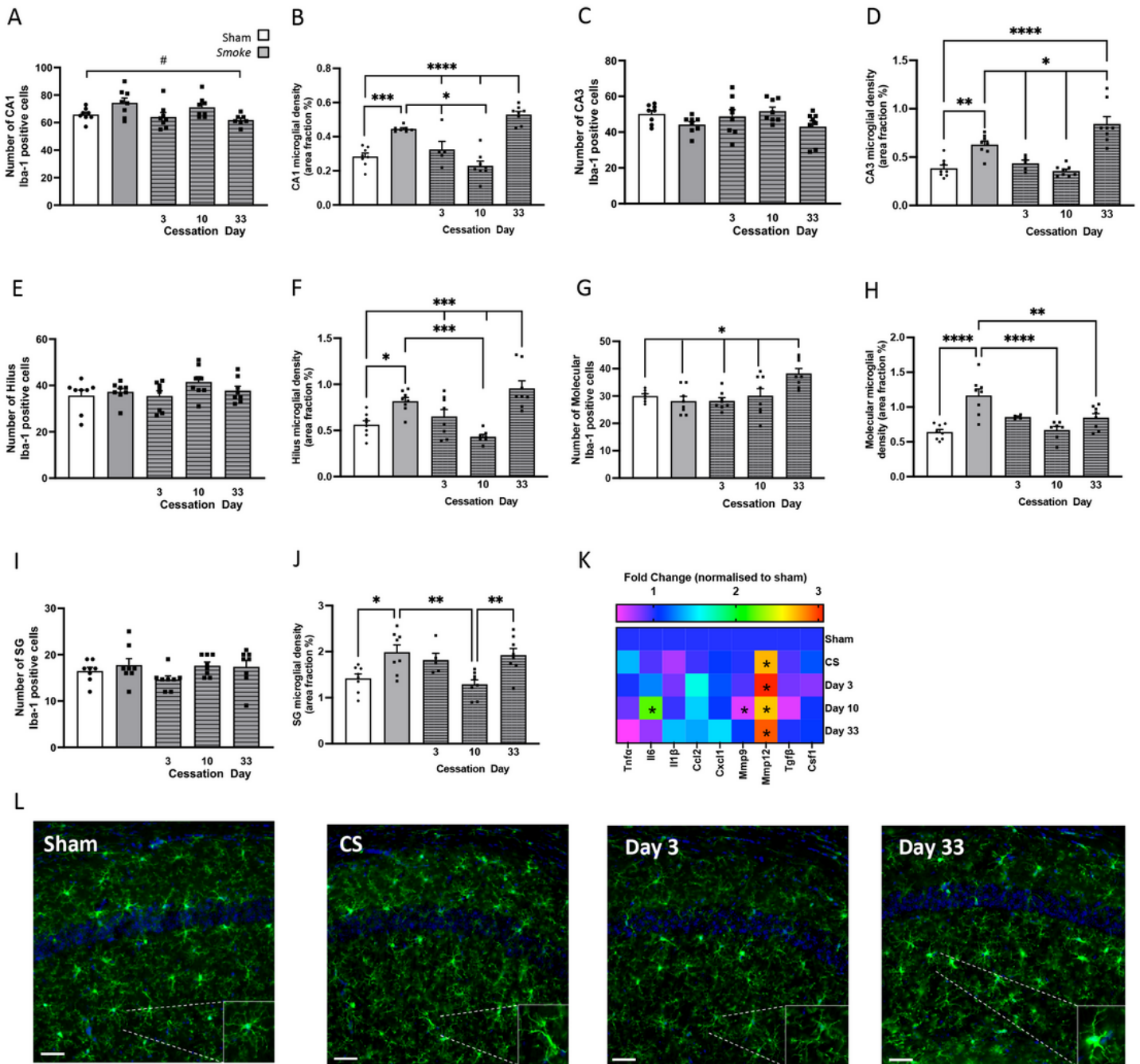


Figure 3

. Cigarette smoke (CS) cessation alters microglial morphology. Microglial area per cell were increased throughout the hippocampus by CS exposure and microglia were further exacerbated 33 days after smoke cessation. (A-J) ionized calcium binding adaptor molecular (Iba-1) labelling through the CA1, CA3,

dentate gyrus (DG) hilus, DG molecular and DG subgranular / granular regions of the hippocampus. (A, B) CA1 (Number: $F(4,34) = 3.652$, $p = 0.0140$; Area per cell: $F(4,31) = 28.55$, $p < 0.0001$); (C, D) CA3 (Area per cell: $F(4,32) = 20.84$, $p < 0.0001$); (E, F) Dentate gyrus hilus (Area per cell: $F(4,34) = 11.96$, $p < 0.0001$); (G, H) molecular (Number: $F(4,34) = 5.725$, $p = 0.0012$; Area per cell: $F(4,30) = 11.63$, $p < 0.0001$); (I, J) subgranular / granular (Area per cell: $F(4,32) = 6.222$, $p = 0.0008$). (K) Gene expression of cytokines and chemokines in the hippocampus (Il6: $F(4,28) = 3.086$, $p = 0.0318$; Mmp9: $F(4,27) = 6.152$, $p = 0.0012$; Mmp12: $F(4,28) = 2.855$, $p = 0.042$). (L) Representative photomicrographs of the CA1 from room air (sham) and CS-exposed mice illustrating differences in area per cell of Iba-1-stained cells. Scale bars = $50\mu\text{m}$. Data are expressed as mean + SEM ($n = 5 - 8$ per group). # $p < 0.05$ effect of exposure; * $p < 0.05$; ** $p < 0.01$; *** $p < 0.001$; **** $p < 0.0001$.

Figure 4

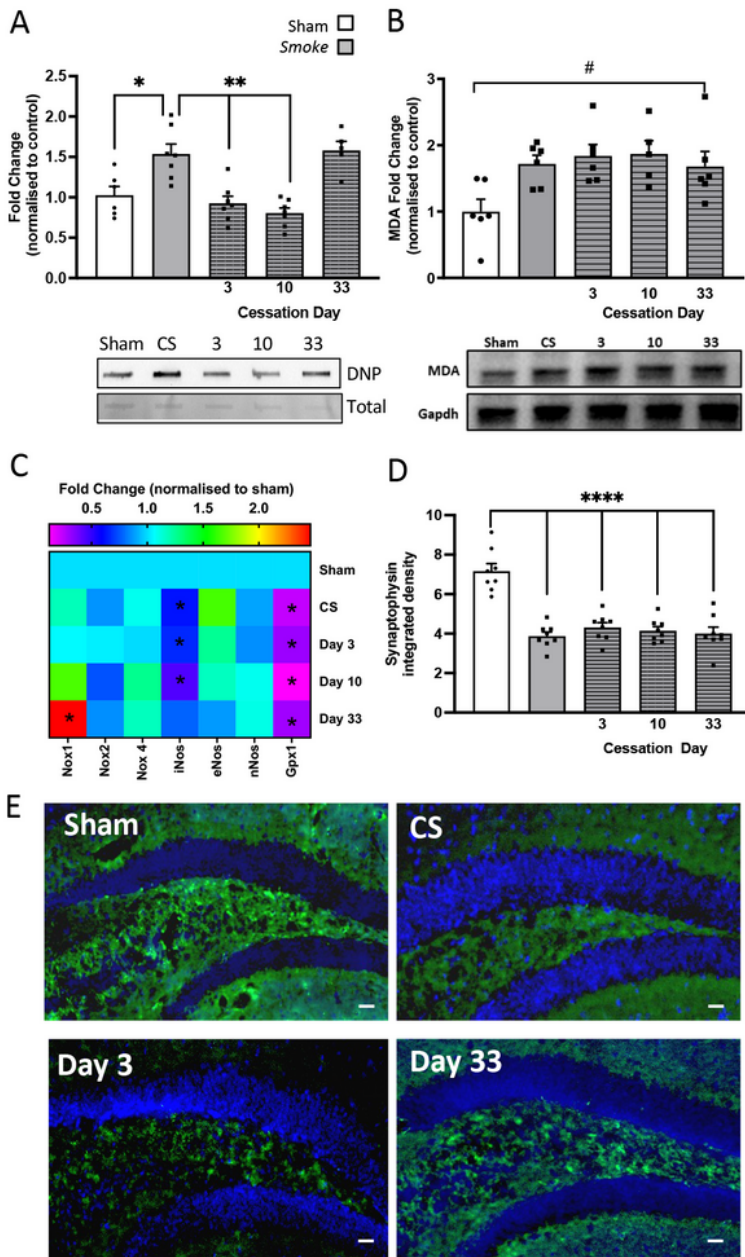


Figure 4

Cigarette smoke (CS) cessation increases hippocampal oxidative stress. (A) protein carbonylation ($F(4,27) = 12.55, p < 0.0001$); (B) lipid peroxidation ($F(4,24) = 3.721, p = 0.0171$); (C) Gene expression of oxidative markers in the hippocampus (Nox1: $F(4,24) = 4.263, p = 0.0084$; Nox4: $F(4,28) = 9.330, p < 0.0001$; iNos: $F(4,29) = 4.474, p = 0.0061$; Gpx1: $F(4,25) = 20.82, p < 0.0001$; $n = 6$ per group). (D) Synaptophysin labelling in the dentate gyrus (DG) hilus region of the hippocampus ($F(4,35) = 23.88, p <$

0.0001; n = 7-8 per group). (E) Representative photomicrographs of the DG hilus from room air (sham) and CS-exposed mice illustrating differences in synaptophysin density. Data are expressed as mean + SEM. # p < 0.05 main effect of exposure; * p = 0.05; ** p < 0.01, **** p < 0.0001.

Figure 5

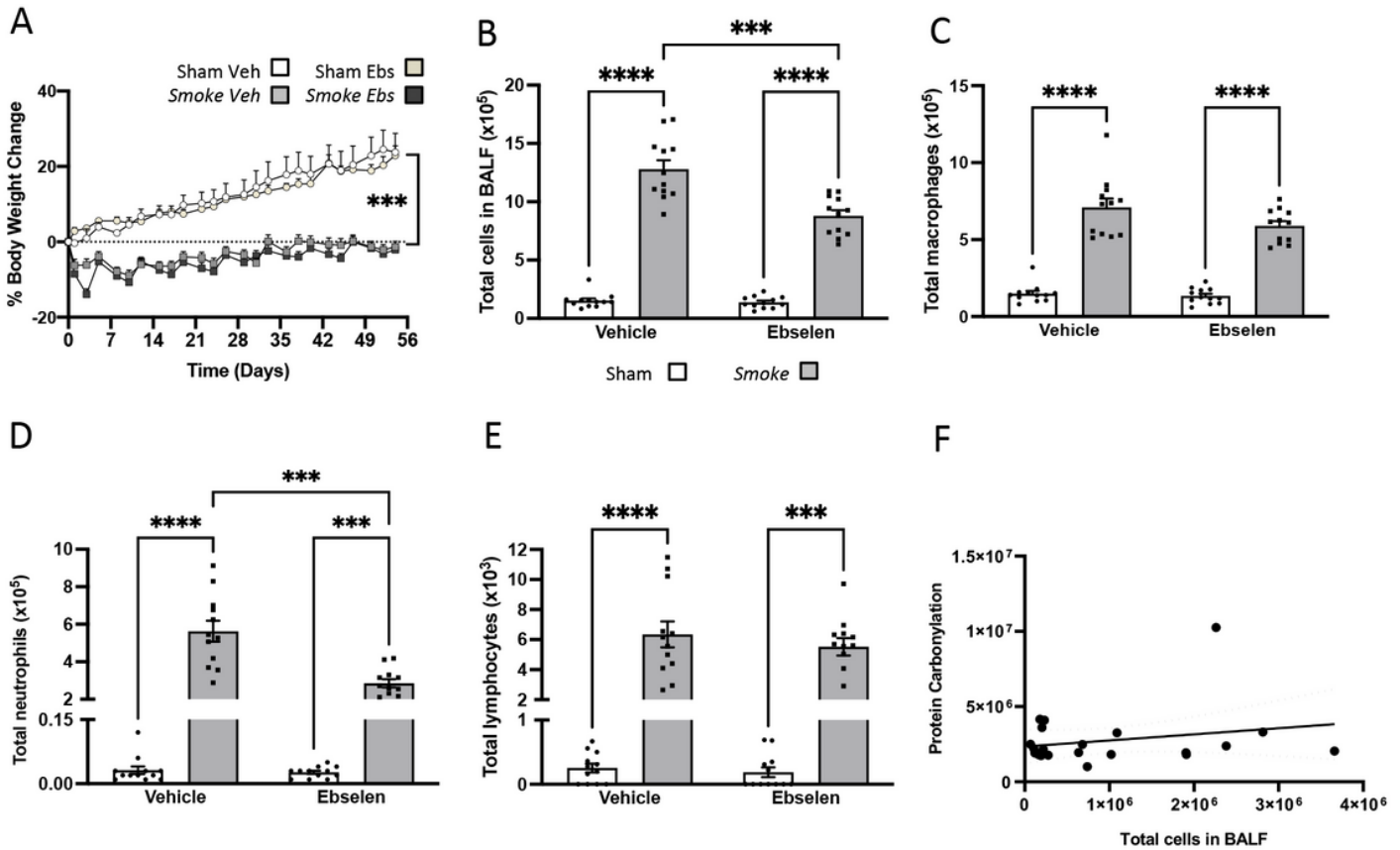


Figure 5

Cigarette smoke (CS)-induced bronchoalveolar lavage fluid (BALF) cellularity was partially reversed by ebselen treatment. Mice were exposed to CS or room air (sham) concomitant with ebselen treatment for 8 weeks. (A) body weight percentage change (n = 12 per group). (B) Total number of cells (interaction between exposure and treatment: $F(1,11) = 20.88$, $p = 0.0008$) (C); macrophages (main effect of exposure: $F(1,11) = 246.5$, $p < 0.0001$) (D); neutrophils (interaction between exposure and treatment: $F(1,11) = 19.57$, $p = 0.0001$) (E); and lymphocytes (main effect of exposure: $F(1,11) = 173.9$, $p < 0.0001$) in BALF (n = 12 per group). (F) BALF protein carbonylation ($r(20) = 0.0523$, $p = 0.306$; n = 12 per group). Data are expressed as mean + SEM. *** p < 0.001, **** p < 0.0001.

Figure 6

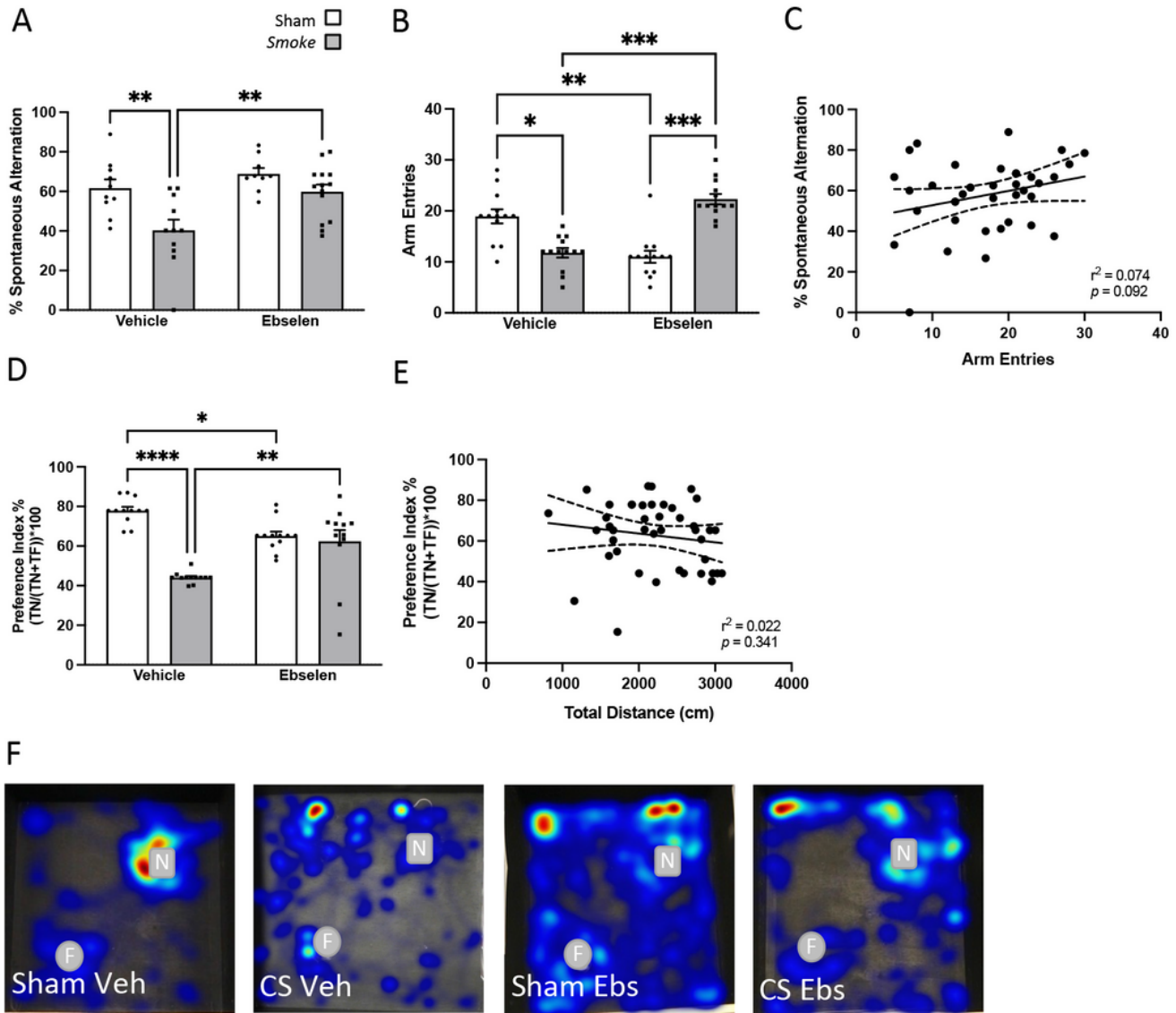


Figure 6

Prophylactic ebselen treatment reverses hippocampal-dependent memory impairments. (A) spontaneous alternation percentage in Y-maze (significant effect of exposure: $F(1,23) = 22.60$, $p < 0.0001$; significant effect of treatment: $F(1,23) = 9.792$, $p = 0.0047$; $n = 7 - 11$); (B) Y-maze arm entries (significant interaction between exposure and treatment: $F(1,12) = 44.56$, $p < 0.0001$); (C) correlation between arm entries and spontaneous alternation in Y-maze ($r(37) = 0.074$, $p = 0.092$); (D) novel objection recognition

(NOR) task preference index ($F(1,11) = 29.48, p = 0.0002, n = 7 - 9$); (E) correlation between preference index and total distance (cm) in mice exposed to room air (sham), smoke and / or vehicle or ebselen ($r(41) = 0.022, p = 0.341$); (F) heatmaps illustrating familiar object (circle) and novel object (square) exploration in the NOR. Heat maps were generated in Ethovision using the over-heatmap setting allowing comparison between the representative animals. Data are expressed as mean + SEM. * $p < 0.05$; ** $p < 0.01$; *** $p < 0.001$; **** $p < 0.0001$.

Figure 7

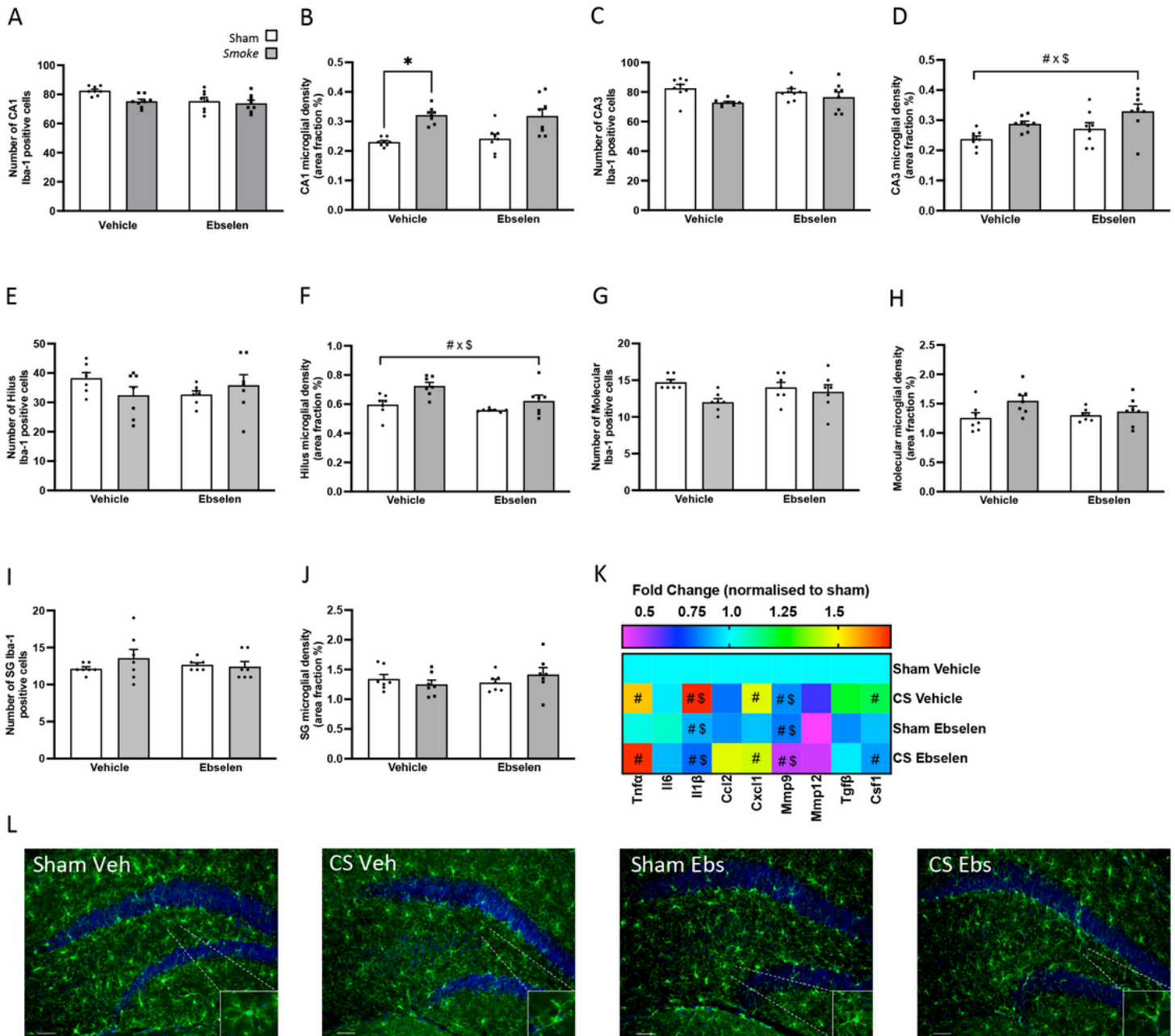


Figure 7

Prophylactic ebselen treatment does not reverse hippocampal microglial profile. (A-J) ionized calcium binding adaptor molecular (Iba-1) labelling through the CA1, CA3, dentate gyrus (DG) hilus, molecular and subgranular / granular regions of the hippocampus. (A, B) CA1 (Area per cell: main effect of exposure: $F(1,7) = 45.45$, $p = 0.0002$; $n = 5-8$ per group); (C, D) CA3 (Area per cell: main effect of exposure: $F(1,7) = 45.06$, $p = 0.0003$ and main effect of treatment: $F(1,7) = 6.164$, $p = 0.042$); (E, F) DG hilus (Area per cell: main effect of exposure: $F(1,6) = 6.902$, $p = 0.039$ and main effect of treatment: $F(1,7) = 24.15$, $p = 0.002$); (G, H) molecular; (I, J) subgranular. (K) Gene expression of cytokines and chemokines in the hippocampus (Il6: $F(4,28) = 3.086$, $p = 0.0318$; Mmp9: $F(4,27) = 6.152$, $p = 0.0012$; Mmp12: $F(4,28) = 2.855$, $p = 0.042$; $n = 6$ per group). (L) Representative photomicrographs of the CA1 from room air (sham) and cigarette smoke-exposed mice illustrating differences in area per cell of Iba-1-stained cells. Scale bars = 50 μ m. Data are expressed as mean + SEM. # $p < 0.05$ main effect of exposure; \$ $p < 0.05$ main effect of treatment.

Figure 8

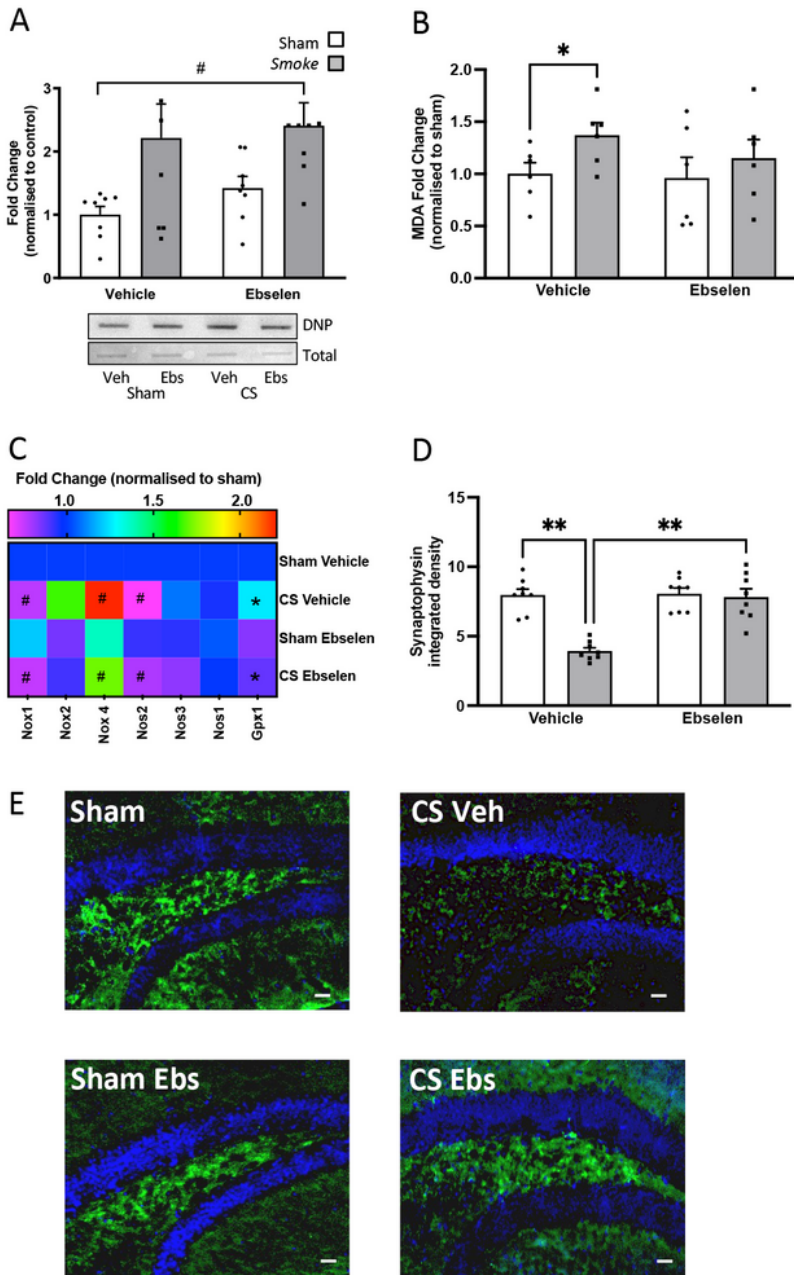


Figure 8

Ebselen prevents cigarette smoke (CS)-induced synaptophysin deficits. (A) protein carbonylation (main effect of exposure: $F(1,28) = 10.26$, $p = 0.0034$; $n = 6$ per group); (B) lipid peroxidation (main effect of exposure: $F(1,5) = 12.37$, $p = 0.018$; $n = 6$ per group); (C) Gene expression of oxidative markers in the hippocampus (Nox1: main effect of exposure: $F(1,5) = 350.46$, $p = 0.0019$; Nox4: (main effect of exposure: $F(1,5) = 6.819$, $p = 0.0476$); Nos2: (main effect of exposure: $F(1,5) = 9.311$, $p = 0.0028$; Gpx1:

main effect of treatment: $F(1,5) = 29.72$, $p = 0.0028$; $n = 6$ per group). (D) Synaptophysin labelling in the dentate gyrus hilus region of the hippocampus ($F(1,7) = 17.42$, $p = 0.0042$; $n = 7-8$ per group). Data are expressed as mean + SEM. # $p < 0.05$ main effect of exposure; * $p < 0.05$; ** $p < 0.01$.

Supplementary Files

This is a list of supplementary files associated with this preprint. Click to download.

- [SupplementaryTable1.docx](#)